University of Groningen

Mechanistic study of visible light-driven CdS or g-C$_3$N$_4$-catalyzed C–H direct trifluoromethylation of (hetero)arenes using CF$_3$SO$_2$Na as the trifluoromethyl source

Wang, Lele; Liu, Ming; Zha, Wenying; Wei, Yingcong; Ma, Xiongfeng; Xu, Chunwang; Lu, Chenggang; Qin, Nanfang; Gao, Li; Qiu, Wenzhao

IMPORTANT NOTE: You are advised to consult the publisher's version (publisher's PDF) if you wish to cite from it. Please check the document version below.

Document Version
Publisher's PDF, also known as Version of record

Link to publication in University of Groningen/UMCG research database

Mechanistic study of visible light-driven CdS or g-C$_3$N$_4$-catalyzed C—H direct trifluoromethylation of (hetero)arenes using CF$_3$SO$_2$Na as the trifluoromethyl source

Lele Wang [a], Ming Liu [a], Wenying Zha [a,b], Yingcong Wei [a], Xiongfeng Ma [a], Chunwang Xu [a], Chenggang Lu [a], Nanfang Qin [a], Li Gao [c], Wenzhao Qiu [a], Rongjian Sa [b,*], Xianzhi Fu [a], Rusheng Yuan [a,*]

[a] State Key Laboratory of Photocatalysis on Energy and Environment, Fuzhou University, Fuzhou 350108, Fujian, China
[b] Institute of Oceanography, Fujian Key Laboratory of Functional Marine Sensing Materials, Minjiang University, Fuzhou, Fujian 350108, China
[c] Department of Pharmacy, University of Groningen, Deusinglaan 1, 9700 AV Groningen, Netherlands

ARTICLE INFO

ABSTRACT

The mild and sustainable methods for C—H direct trifluoromethylation of (hetero)arenes without any base or strong oxidants are in extremely high demand. Here, we report that the photo-generated electron-hole pairs of classical semiconductors (CdS or g-C$_3$N$_4$) under visible light excitation are effective to drive C—H trifluoromethylation of (hetero)arenes with stable and inexpensive CF$_3$SO$_2$Na as the trifluoromethyl (TFM) source via radical pathway. Either CdS or g-C$_3$N$_4$ propagated reaction can efficiently transform CF$_3$SO$_2$Na to ·CF$_3$ radical and further afford the desired benzotrifluoride derivatives in moderate to good yields. After visible light initiated photocatalytic process, the key elements (such as F, S and C) derived from the starting TFM source of CF$_3$SO$_2$Na exhibited differential chemical forms as compared to those in other oxidative reactions. The photogenerated electron was trapped by chemisorbed O$_2$ on photocatalysts to form superoxide radical anion (O$_2^{·-}$) which will further attack ·CF$_3$ radical with the generation of inorganic product F$^-$ and CO$_2$. This resulted in a low utilization efficiency of ·CF$_3$ (<50%). When nitro aromatic compounds and CF$_3$SO$_2$Na served as the starting materials in inert atmosphere, the photoexcited electrons can be directed to reduce the nitro group to amino group rather than being trapped by O$_2$. Meanwhile, the photogenerated holes oxidize SO$_2$CF$_3^-$ into ·CF$_3$. Both the photogenerated electrons and holes were engaged in reductive and oxidative paths, respectively. The desired product, trifluoromethylated aniline, was obtained successfully via one-pot free-radical synthesis.

© 2020 Elsevier Inc. All rights reserved.

1. Introduction

Trifluoromethyl (TFM) compounds are core building blocks in the fields of pharmaceutical, organic synthesis, and agrochemical, since the TFM group can dramatically influence their properties (such as membrane permeability and bioavailability, elevated electronegativity and oxidation resistance) [1–6]. Thus, it has gained a noteworthy rise of interest for the incorporation of a —CF$_3$ moiety into organic molecules [7]. Among the diverse synthetic methodologies to construct C—C bonds [8,9], photocatalytic C—H bond direct trifluoromethylation of (hetero)arenes has been one of the most sustainable and mildest ways as it avoids the involvement of pre-functionalized substrates and harsh reaction conditions [10–17]. In recent years, effective visible-light catalysts, with outstanding photocatalytic performance, including homogeneous metal complexes [18] ([Ru(bpy)$_3$Cl$_2$] [19], [Co(Ph-tpy)$_2$][(PF$_6$)$_3$] [20], Ir(ppy)$_3$ [21]), organic dyes (methylene blue [22], Eosin Y [23]), quinones [24] and heterogeneous inorganic materials (such as Rh-modified TiO$_2$ NPs) [25] have been developed in the trifluoromethylation reaction. Semiconductor photocatalysts with diverse band structures endowed themselves with great potential for driving this reaction [7,26–27]. However, not much attention is paid to the trifluoromethylation of (hetero)arenes on cheap and classical semiconductors without any metal modification or additives (strong oxidants and precious metals).

The radical trifluoromethylation of (hetero)arenes is an efficient strategy owing to the electrophilic nature of ·CF$_3$ radical with a low-lying singly occupied molecular orbital (SOMO) [28] which was apt to react with electron-rich (hetero)arenes. Compared with TFM metals (M = Cu, Zn, Si, Cd, Sn, Hg and Pb) [29–30] and gaseous CF$_3$I [31], CF$_3$SO$_2$Na as a safe, inexpensive and stable solid TFM

* Corresponding authors.
E-mail addresses: rjsa@mju.edu.cn (R. Sa), yuanrs@fzu.edu.cn (R. Yuan).

source can be easily oxidized to release $\cdot CF_3$ (the lowest potential is 0.6 eV) [24]. Theoretically, visible light responsive photocatalysts absorb incident photons of the valid light wavelength larger than 420 nm which decided by their physical bandgaps, and thus generate (oxidative potentials) exciton transitions in the valence band (VB) being more positive than 0.6 eV enabling the transformation of CF_3SO_2Na to $\cdot CF_3$. Since the photo-generated excitons is ever in the native form of electron-hole pairs, the separation of these electron-hole pairs to offer more holes for subsequent oxidation step or efficiently utilize electrons synchronously is the most important issue in this light-initiated synthetic reactions [32,33]. In addition, the transfer balance of photo-generated electron-hole pairs and the chemical evolution of the elements in CF_3SO_2Na are essential during photocatalytic trifluoromethylation, but little attention has been paid to it previously.

Herein, we report the application of semiconductors (such as CdS nanorod or $g\text{-}C_3N_4$) as the heterogeneous photocatalysts for the functionalization of (hetero)arenes to synthetize trifluoromethylated (hetero)arenes under visible light irradiation. In this work, a series of benzotrifluoride derivatives were successfully synthesized in good yields, and the experimental fact revealed that the formed O_2^- during the photocatalysis is the key species leading to the unexpected decomposition of $\cdot CF_3$ derived from CF_3SO_2Na. By introducing nitro aromatic compounds as the starting material, the photo-generated electrons tend to reduce nitro group of the compounds to amino group. This would avoid the trapping process of electrons by O_2 and be an effective strategy for one-pot synthesis of trifluoromethylated aniline from nitro aromatic compound.

2. Experimental procedures

2.1. General information

All reagents and solvents are commercially available (Beijing innoChem Science&Technology Co. Ltd.), and they were further dried by the vacuum rotary evaporator to remove all traces of water and then stored in the N_2-filled glovebox. The 10 mL Schlenk tube charged with a magnetic stirrer, which was used as the reactor in the trifluoromethylation reaction. The visible light ($\lambda > 420$ nm) was provided by a 300 W xenon lamp (PLS-SXE300C, Beijing Perfect Light Co.) equipped with an IR-cutoff filter ($\lambda < 780$ nm). UV source was provided by 4-W UV lamp with certain wavelength centered at 365 nm (Philips, TUV 4 W/G4 T5). The LED lights were provided by Beijing Perfect Light Co. (PL-LED100 lamps, centered at 400 ± 15 nm, 420 ± 15 nm, 450 ± 15 nm, 475 ± 15 nm, 500 ± 15 nm, 520 ± 15 nm, 550 ± 15 nm, respectively). The incident light energy was measured with a spectroradiometer (International Light Technologies Model ILT950).

The chemical structures of the products were confirmed by comparison with standard chemicals and GC–MS (Agilent Technologies, GC 7890B, MS 5977A) data. GC equipped with a FID detector (Agilent Technologies, GC 7890B) and a HP-5 5% phenyl methyl siloxane column (30 m × 0.32 mm × 0.5 µm), which was used for the quantifiable measure of trifluoromethoxybenzene. ^1H and ^{13}C NMR spectra were recorded on a Bruker UltraShield Plus Avance III (500 MHz and 125 MHz, respectively). Peaks were referenced to residual solvent ($CDCl_3$, 1H, 7.26 ppm, 13C, 77.0 ppm). The quantitative yields of trifluoromethylated compounds were calculated using ^{19}F NMR with trifluoromethoxybenzene as the internal standard. The ^{19}F NMR spectra were obtained at 293 K on a Bruker Avance 500 spectrometer (400 MHz), and chemical shifts were recorded relatively to the solvent resonance.

The size and morphology of catalysts were measured by a Hitachi New Generation SU8010 field emission scanning electron microscope (FE-SEM, JSM-670 F). The transmission electron micro-

scopy (TEM) images, high-resolution transmission electron microscopy (HRTEM) images (with an acceleration voltage of 200 kV), and selected area fast Fourier transform (FFT) pattern were measured on a JEOL JEM-3000F microscope, which with a CCD camera as the detector. The Brunauer-Emmett-Teller (BET) surface area and the pore size distribution curve of catalysts were analyzed by a Micromeritics ASAP 2020 surface area analyzer. The X-ray photoelectron spectra (XPS) were acquired using a Thermo Scientific EscaLab 250 XPS system with a monochromatic Al Kα source and a charge neutralizer. The background pressure was maintained at $< 10^{-6}$ Pa during data acquisition. The binding energies were referenced to the hydrocarbon C1s energy of 284.8 eV from adventitious carbon. A Varian Cary 500 UV–Vis spectrophotometer was used to record the UV–Vis diffuse reflectance spectra (DRS) of various solid samples. The photoelectrochemical characterization was performed on a Metrohm-Autolab AUT302N Electrochemical workstation. Photocurrent measurements were carried out in a typical three-electrode configuration with an Ag/AgCl electrode, a coiled Pt wire as the reference and counter electrode, respectively. X-ray diffraction (XRD) studies of catalyst were carried out with a Bruker D8 Advance instrument. The electron paramagnetic resonance (EPR) experiments were carried out on Bruker A300 instrument operating in the X-band at room temperature. An ion chromatograph (Dionex ICS-1100, Dionex) equipped with a conductivity detector and an ion exchange column (IonPac AS11-HC, Dionex) was used to detect and quantify F^-.

2.2. Catalyst preparation

Synthesis of CdS nanorods. In a typical preparation process, $CdCl_2 \cdot 2.5H_2O$ (4.62 g, 0.023 mol), thiourea (CH_4N_2S, 4.62 g, 0.061 mol) and a given amount of ethylenediamine (60 mL) were added into a 100 mL Teflon-lined stainless steel autoclave. The solution was stirred at room temperature for 1 h, and then heated to 160 °C for 24 h. When it cooled to room temperature naturally, the product was washed with distilled water and absolute ethanol several times to remove the excess reactants and byproduct. Finally, the sample was dried in a vacuum oven at 60 °C for 8 h.

Synthesis of $g\text{-}C_3N_4$. Typically, it was synthesized thermally by heating urea (10 g) at 550 °C for 2 h with a heating rate of 2 °-C min^{-1} under ambient pressure in air. Then, the as-obtained yellow powder was collected and grinded to get the final sample.

Synthesis of $CdS/g\text{-}C_3N_4$. Pre-weighed CdS and $g\text{-}C_3N_4$ were added into the appropriate ethanol-water mixture (Volume ratio, 1:1). After ultrasonic treatment for 2 h, the mixture was stirred and dried at 60 °C in an oil bath. Then the obtained powders were calcined at 300 °C in air with a heating rate of 15 °C/min for 2 h. Finally, the bright yellow product was collected for further characterization. The synthesized $CdS/g\text{-}C_3N_4$ composites are denoted as CS-x, and × represents the theoretical concentration of $g\text{-}C_3N_4$ (x wt.%). For example, the 20 wt% $g\text{-}C_3N_4$/80 wt% CdS catalyst can be denoted as CS-80 (Table S1).

2.3. General procedures for the photocatalytic trifluoromethylation of (hetero)arenes

In a typical photocatalytic experiment, benzene (11.2 mmol), CH_3CN (1 mL), photocatalyst (10 mg) and CF_3SO_2Na (0.5 mmol) were mixed in the reactor in a N_2-filled glovebox. The mixture was stirred upon 500 nm LED light irradiation for 12 h. Then the resulting mixture was centrifuged and the supernatant was preliminarily analyzed by GC, GC–MS and ^{19}F NMR techniques. All the other photoinduced trifluoromethylation reactions of (hetero) arenes undergo similar procedures as mentioned above.

2.4. Typical procedure for the thermal reactions

The procedures for thermal reactions of (hetero)arenes and CF_3-SO_2Na are similar to those for the photoreactions while the reaction temperature was controlled by a heating jacket at 60 °C under dark conditions.

2.5. Detection of free radicals

Electron paramagnetic resonance spectroscopy (EPR) was used to monitor the species of free radicals with a Bruker A300 instrument. Typically, for the detection of O_2^-, a solution containing CdS (0.07 mmol), CH_3CN (1 mL) and DMPO (5, 5-dimethyl-1-pyrroline N-oxide, 0.1 mmol) was sucked by a capillary tube. One end of it was plugged with plasticine and the capillary tube was then placed into a sealed quartz tube under N_2 atmosphere. The quartz tube was irradiated with visible light irradiation and the spectra were recorded in situ.

The detection for $\cdot CF_3$ experienced the same procedures as that of O_2^-, except that MNP (2-methyl-2-nitrosopropane dimer, 0.1 mmol/mL) was used as the radical scavenger. The sample was prepared by mixing CF_3SO_2Na (0.2 mmol/mL) with acetonitrile (1 mL).

2.6. Procedure of KIE experiment between benzene and C_6D_6

A 10 mL Schlenk tube was charged with benzene (5.6 mmol), C_6D_6 (5.6 mmol), CH_3CN (1 mL) and CF_3SO_2Na (0.5 mmol). The resulting mixture was stirred upon visible light (420–780 nm) irradiation for 12 h. The crude mixture was then centrifuged and the supernatant was preliminarily recorded on ^{19}F NMR.

2.7. Computational details

The proposed reaction path for trifluoromethylation reaction catalyzed by g-C_3N_4 has been studied by Density Functional Theoretical (DFT) methods, which were implemented in DMol^3 package [34–35]. The generalized gradient approximation (GGA) with the functional of Perdew-Burke-Ernzerhof (PBE) was utilized for all calculations. The double-numeric quality basis set to expand wave functions with polarization functions (DNP) was adopted. The Grimme's scheme (D2) to treat the long- range dispersion interactions [36]. A Fermi smearing of 0.005 hartree was utilized in this calculation, and a size of $2 \times 2 \times 1$ was used for structural relaxation. The convergence criteria for energy, gradient and displacement convergence were 1.0×10^{-5} Ha, 0.002 Ha/Å, and 0.005 Å, respectively. All periodic slabs had a vacuum spacing of at least 15 Å, which was thick enough to avoid artificial interaction. A Γ-centered $4 \times 4 \times 3$ Monkhorst-Pack grid for the Brillouin zone sampling was used in our calculations. The adsorption energies (ΔE_{ads}) with zero-point-corrected are defined using the equation $\Delta E_{ads} = [E_{slab+adsorbate} - (E_{slab} + E_{adsorbate})] + \Delta ZPE_{ads}$, where $E_{slab} +$-$E_{adsorbate}$, E_{slab} and $E_{adsorbate}$ represent the total energy of the slab covered with the adsorbate, the energy of the bare slab and the energy of the free adsorbate molecules, respectively. ΔZPE_{ads} represents the zero-point vibrational energy (ZPE) correction for the adsorption.

3. Results and discussion

3.1. Photoinduced trifluoromethylation of (Hetero)Arenes

Initially, a series of semiconductors (such as CdS, g-C_3N_4, BiVO$_4$, Ag$_3$PO$_4$ and WO$_3$) possessing high visible light absorption ability (>420 nm) were chosen as the photocatalysts to investigate their photocatalytic performance in the trifluoromethylation reaction of benzene (Fig. 1a). The corresponding band structures of these semiconductors showed that the VB positions are more positive than 0.6 eV, which theoretically enable these semiconductors to be a possible contributor in affording $\cdot CF_3$ radicals from CF_3SO_2Na (Fig. 1b) [37]. However, when the reaction mixture (2-methyl-2-nitrosopropane (MNP) as a trapping agent) was irradiated with visible light (420–780 nm, Fig. 1c), only CdS and g-C_3N_4 could give a singlet–triplet splitting signal at g = 2.0061 ($\alpha_N = \alpha_F = 12.25$ G), which can be attributed to MNP-CF_3 adduct [23]. Furthermore, the intensity of this signal increased with a prolonged irradiation time in the CdS catalyzed system, confirming the generation of $\cdot CF_3$ via the oxidation of CF_3SO_2Na. The trifluoromethylation reaction proceeded smoothly only in the presence of CdS or g-C_3N_4, affording 49.2% or 36.8% yield of benzotrifluoride (**3a**) under visible light irradiation (Table 1, entries 1–6). When the scavengers of holes (Na$_2$SO$_3$) were added into the CdS reaction system, the trifluoromethylation reaction was almost terminated. This means that photogenerated holes are solely responsible for the trifluoromethylation (Table entry 7). These above results suggest that the VB positions and band gaps were not the sole factors determining the effectiveness of semiconductors in the trifluoromethylation reaction.

To further investigate the reason, we conducted the trifluoromethylation reactions employing CdS as the model catalyst. As shown in Table 1, no **3a** product was observed in the absence of photocatalyst or light, even upon heating to 60 °C, suggesting that a photocatalytic process was involved in this reaction (entries 8–10). The transformation process could not occur in the absence of O_2, indicating that O_2 may play an important role in the occurrence of this reaction (entry 10). Generally, when O_2 as the essential substance in the reaction system, it could be reduced to superoxide radical anion (O_2^-) by the semiconductors which has negative enough CB positions (<-0.33 eV) under light irradiation (Fig. 1b). Thus, we reason that, in the case of O_2 the photo-generated electrons can be trapped by O_2 when the semiconductors possess negative enough CB positions than -0.33 eV [38]. This speculation was then testified by the EPR spectra of O_2^-, in which characteristic signals for DMPO-O_2^- adducts were observed when acetonitrile solution containing CdS or g-C_3N_4 (with 5,5-dimethyl-1-pyrroline N-oxide (DMPO) as the trapping agent) was irradiated by visible light (Fig. 1d). Similarly, the signal intensity increases with the irradiation time. No O_2^- signal was obtained in the presence of BiVO$_4$, Ag$_3$-PO$_4$ or WO$_3$ [39]. This trend was in good agreement with the experimental result of these semiconductors in the trifluoromethylation reaction. Thus, we rationally concluded that O_2 as an electron trapping agent prevented the fast recombination of electrons and holes, benefitting the formation of **3a**.

Inspired by these initially promising results, we further explored the effects of different variables on the activity of CdS. Upon irradiation with a 500 nm LED light with a lower intensity, nearly no significant decrease in the yield of **3a** (42%) was observed (Table 1, entry 11). Even household CFL lamp could promote the reaction and gave a moderate yield of 23.6% (entry 12). As a substitute for CH_3CN, other solvents such as CH_3OH, EtOH, acetone, DMSO and THF could also promote the reaction in moderate yields which were slightly lower than that of CH_3CN (Fig. 2a). Surprisingly, the introduction of base or acid such as K$_2$HPO$_4$, K$_2$CO$_3$, CH$_3$-COOH, CF$_3$COOH into the reaction resulted in a decrease in the yield of **3a**, suggesting that the additives were not needed for a higher yield of benzotrifluoride (Fig. 2b). As shown in Fig. 2c, the amount of **3a** linearly increased with both the increasing light intensity and the prolonged irradiation time. The dependence of apparent quantum yields (AQYs) on the wavelength of excitation light in this reaction was further investigated. As shown in Fig. 2d, the trend of AQYs at different wavelengths matched well
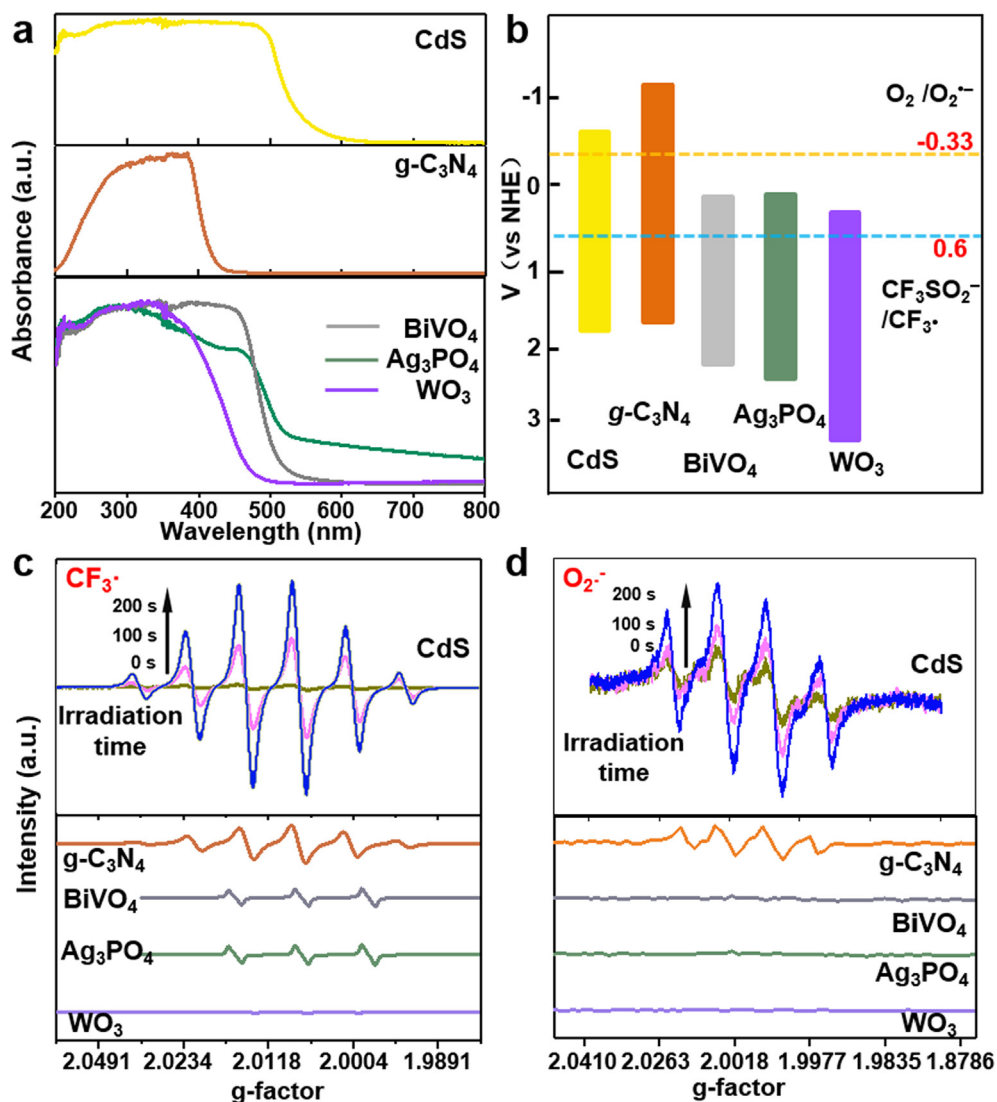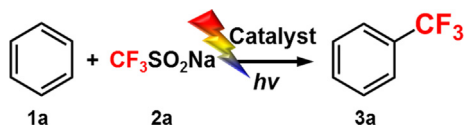
Fig. 1. UV–vis DRS spectra (a) and the band structures (b) of semiconductors. ESR spectra of trifluoromethyl radicals (c) and super oxide anion (d).

Table 1
Photocatalytic C-H direct trifluoromethylation of benzene.

Entry	Condition	Photocatalyst	Amount of 3a (μmol)	Yield (%)
1[a]	420–780 nm	CdS	246	49.2
2	420–780 nm	g-C$_3$N$_4$	184	36.8
3	420–780 nm	BiVO$_4$	×	×
4	420–780 nm	Ag$_3$PO$_4$	×	×
5	420–780 nm	WO$_3$	trace	trace
6	420–780 nm	none	×	×
7[b]	420–780 nm	CdS	trace	trace
8	Dark	CdS	×	×
9	60 °C	CdS	×	×
10[c]	420–780 nm	CdS	×	×
11[d]	500 nm	CdS	210	42.0
12[e]	Household light	CdS	118	23.6

[a] Reaction conditions: 1a (11.2 mmol, 22.4 equiv), 2a (0.5 mmol, 1 equiv), CH$_3$CN (1 mL), photocatalyst (10 mg), room temperature (25 °C), air atmosphere (0.1 MPa), irradiation time (24 h), GC yields (Yield = the molar ratio of benzotrifluoride to initial CF$_3$SO$_2$Na), "×" means not detected. Light intensity (500 mW/cm^2).

[b] Na$_2$SO$_3$ is added in the reaction system.

[c] N$_2$ atmosphere.

[d] Light intensity (80 mW/cm^2).

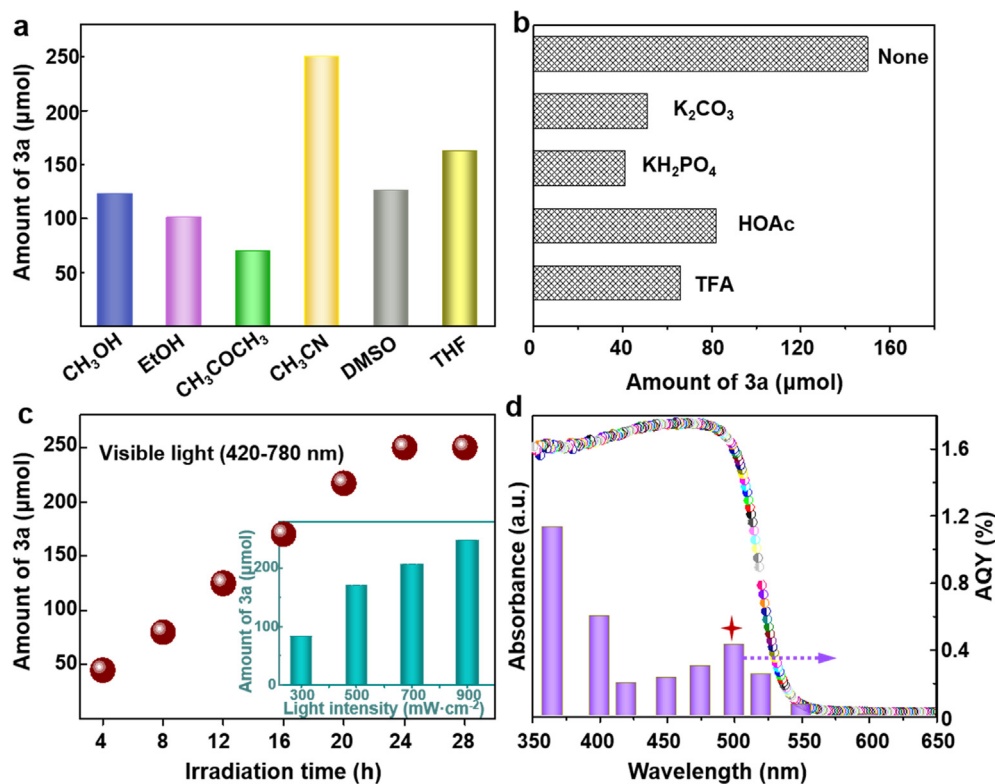[e] Light intensity (20 mW/cm^2, λ = 380–700 nm).

Fig. 2. (a) Yields of **3a** in different solvents. (b) The influence of base or acid (0.25 mmol) on the amount of **3a** irradiated for 14 h. (c) The influence of irradiation time and light intensity (inset, illumined for 16 h) on the amount of **3a**. (d) AQYs at different single-wavelengths and the UV–Vis spectrum of CdS.

with that of the absorption spectra. The highest AQY (0.43%) of CdS was obtained at 500 nm within the visible light range. The longest wavelength available for the reaction has been extended to 550 nm which corresponds to the absorption edge of the catalyst. When 600 nm LED light was used, no product was obtained. The effective wavelength range is compatible with the absorption spectrum of CdS, further indicating that the photo-generated holes over CdS are responsible for the trifluoromethylation of benzene.
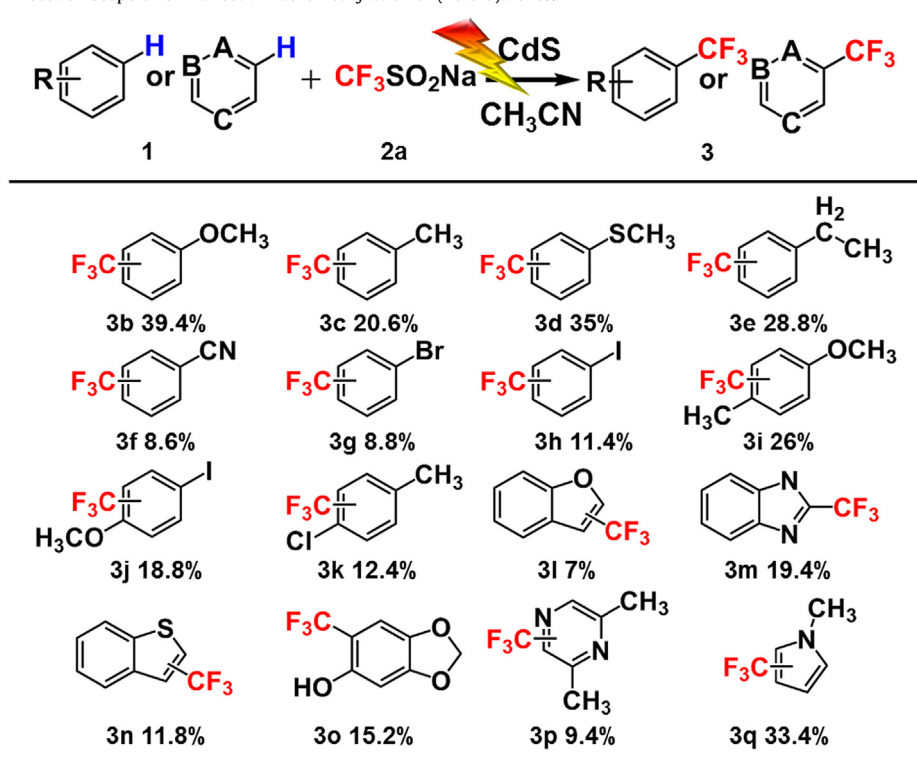
The scope of this trifluoromethylation reaction was successfully extended to a wide variety of (hetero)arenes (Table 2). Most of the employed aromatic substrates could gave moderate yields of target products. When benzene ring bearing electron-donating substituents (such as —OMe, —Me, —SMe and —Et) gave higher yields than that bearing the electron-withdrawing ones (—CN, —I, —Br, **3b-h**), and the yields of desired products increased with the enhancement of donor power (or decreased electro-withdrawing power) of substituent groups. This also confirmed that the trifluoromethylation reaction is sensitive to the electronic effect of the substituent group. Interestingly, the liable leaving group such as -I can keep stable during the trifluoromethylation process since no benzotrifluoride was detected when using iodobenzene as the substrate (3 **h**). The trifluoromethylation of disubstituted benzene (**3b**, **3i**, **3j**, **3c**, **3k**) could also take place and give 12.4–39.4% yield of desired products, respectively. Additionally, a wide range of ring substitution and heteroatom protecting groups are well-tolerated affording 7–33.4% yields of target products (**3l-3q**). Five-membered and six-membered heterocycles including benzofuran, benzimidazole, benzothiophene could also be activated and afford the desired trifluoromethylated products which can be potential pharma-cophores. These results suggest that, this heterogeneous photocatalytic system possess good tolerance of functional groups.

3.2. Photocatalyst characterization

The more detailed characterization of the morphologies and microstructures of the photocatalysts were obtained by SEM and TEM measurements. As shown in Fig. 3a, b, rod-like CdS with an average diameter of 40 nm and the length in the range of 200–300 nm was obtained. The high-resolution TEM images (Fig. 3c) in the selected regions of CdS nanorod showed that the sample exhibits good crystalline and clear lattice fringes with an interval of 3.36 Å corresponding to the interatomic distance of hexagonal CdS (0 0 2) [40,41]. The crystal orientation of the single crystalline CdS was also confirmed by the fast Fourier transform (FFT) pattern. The TEM and SEM images of g-C$_3$N$_4$ showed that the obtained g-C$_3$N$_4$ samples are aggregated by irregular nanosheets (Fig. 3d–f).

The surface chemical composition and oxidation states of the CdS and g-C$_3$N$_4$ samples were further monitored by XPS measurement. As shown in Fig. 4a, the survey spectrum of the elemental composition for CdS confirmed that it was composed of Cd and S elements. The peaks at 404 eV and 410.8 eV in the high-resolution XPS spectrum of the Cd element can be assigned to Cd 3d$_{3/2}$ and Cd 3d$_{5/2}$, respectively (Fig. 4b), [42]. The 6.7 eV difference between these two peaks confirmed the Cd^{2+} states. The peaks at 160.5 eV and 161.5 eV in Fig. 4c correspond to S 2p transitions. The g-C$_3$N$_4$ is comprised of C and N elements as evidenced in the survey spectrum (Fig. 4d). The high-resolution spectrum of the C element showed two peaks at about 284.6 eV and 287.9 eV, which were ascribed to the C in C-C and the sp^2-bonded C in C=N, respectively (Fig. 4e) [43]. As shown in Fig. 4f, the N1s spectrum could be deconvoluted into three peaks centered at 398.4, 400 and 400.5 eV, respectively. The peak at 398.4 eV was assigned to the N in the sp^2 C=N bond and the peaks at 400 and 400.9 eV were corresponding to the N atoms bounded to three C atoms. These results were similar to that of the literature [44].

Table 2
Reaction scope of C-H direct trifluoromethylation of (hetero)arenes.

3b 39.4%   3c 20.6%   3d 35%   3e 28.8%

3f 8.6%   3g 8.8%   3h 11.4%   3i 26%

3j 18.8%   3k 12.4%   3l 7%   3m 19.4%

3n 11.8%   3o 15.2%   3p 9.4%   3q 33.4%

Reaction conditions: 1 (0.2 mL), 2a (0.5 mmol), CH_3CN (1 mL), photocatalyst (10 mg), air atmosphere, light intensity (80 mW/cm^2, λ = 500 nm), irradiation time (24 h), room temperature (25 °C), air atmosphere (0.1 MPa) ^{19}F NMR yields with trifluoromethoxybenzene as internal standard.
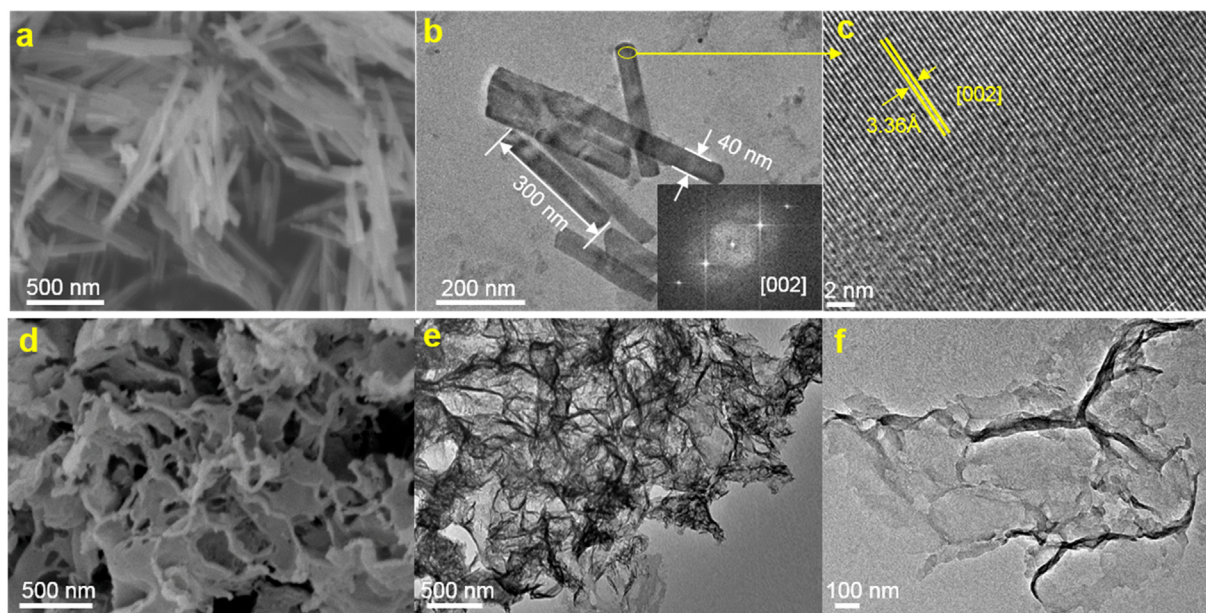

Fig. 3. (a–c) The SEM, TEM and HRTEM images of CdS sample. Inset of (b) is the selected area Fast Fourier transform (FFT) pattern. (d–f) The SEM and TEM images of g-C$_3$N$_4$ sample.

Other physicochemical properties such as pore characteristics and the specific surface area of CdS and g-C$_3$N$_4$ materials were also studied by N$_2$ physisorption measurements (Fig. 4). The BET specific surface area of CdS and g-C$_3$N$_4$ were calculated to be 14.2 m^2/g and 94.1 m^2/g, respectively. This also indicated that the difference in physical adsorptivity of CdS and g-C$_3$N$_4$ was not the major reason resulting in the better performance for CdS in trifluoromethylation of arenes. Further photocurrent spectrum of CdS exhibited a
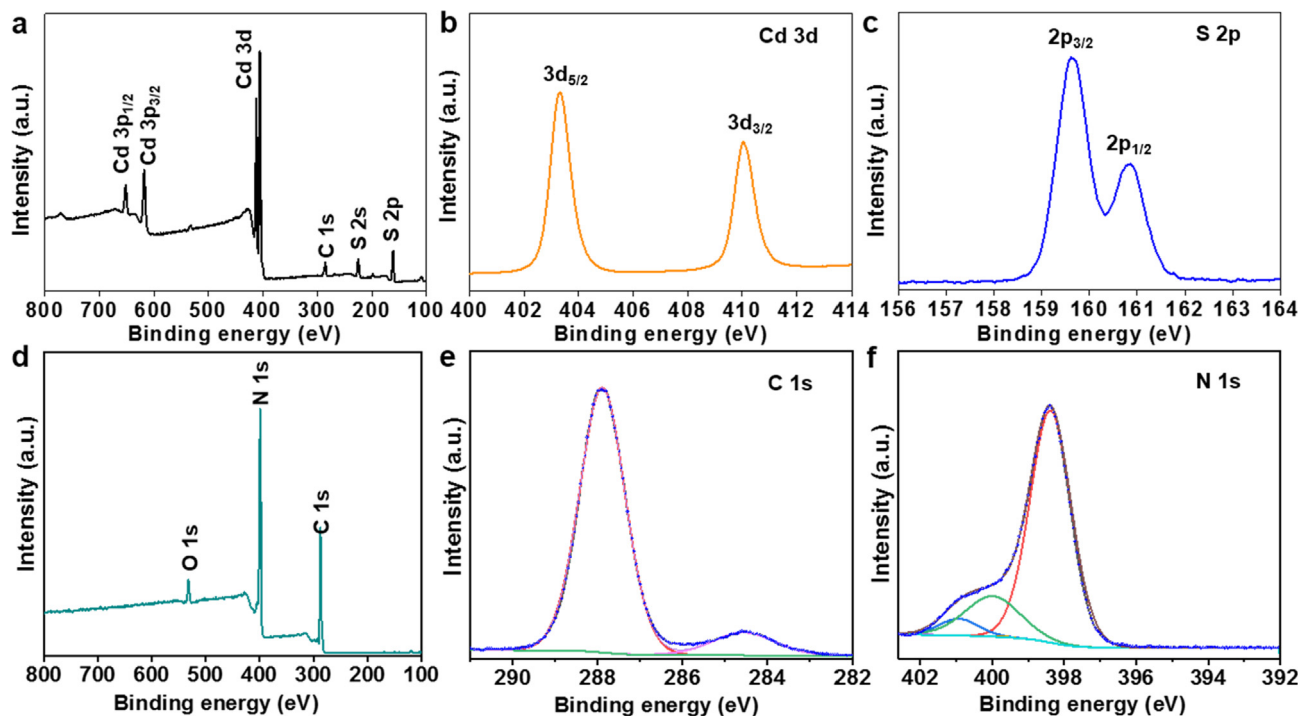
Fig. 4. (a, d) XPS survey spectra of CdS and g-C_3N_4. (b, c, e, f) High resolution XPS spectra of Cd 3d, S 2p, C 1s and N 1s in CdS and g-C_3N_4 samples, respectively.

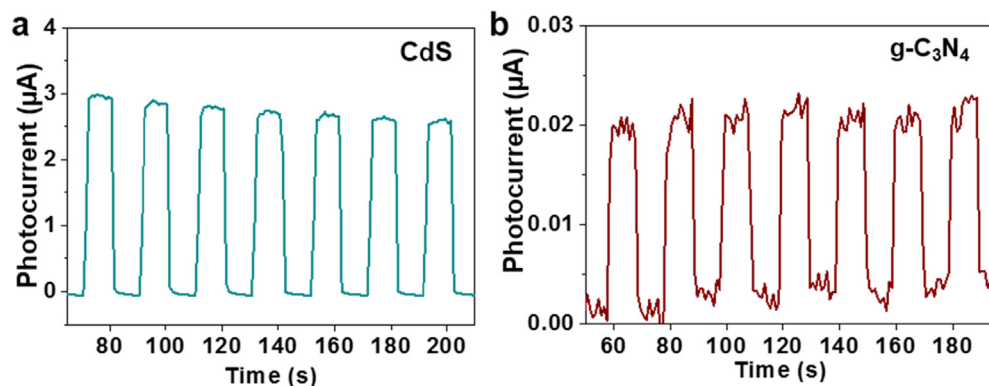**Fig. 5.** Photocurrent spectra of CdS (a) and g-C_3N_4 (b) samples.

higher response compared to that of g-C_3N_4, suggesting better separation ability of the electron-hole pairs (Fig. 5). Considering the preferable photocatalytic performance of CdS under the same reaction conditions, one can conclude that the improved activity of CdS profits from the enhanced visible light absorption and efficient inhibition of the charge carrier recombination. Generally, the separation efficiency of the photoexcited electron-hole pairs will be significantly improved by creating a *p-n* heterojunction at the interface of *p*- and *n*-type semiconductors. This stimulated us to further prepare CdS/g-C_3N_4 composite photocatalyst with joint interface between CdS nanorods and g-C_3N_4 sheets under optimized synthetic condition as shown in Fig. 6a and b (Fig. S1, S2). As expected, the composite catalysts gave significant improvement in the conversion rate of benzotrifluoride as compared to that of pure CdS or g-C_3N_4 sample (Fig. 6c and d). Among all the CdS/g-C_3N_4 composites, CS-60 showed the highest rate. However, the final yield of the trifluoromethylated products with prolonged reaction time for all the composites were still lower than 50% of CF_3SO_2Na (Table S2).

3.3. Cyclic utilization of the photocatalyst

To investigate the stability of CdS and g-C_3N_4 photocatalysts, 5 cycles of photocatalyzed trifluoromethylation were conducted. As shown in Fig. 7a, there is almost no obvious decrease in the yield of **3a** after 5 reaction cycles using g-C_3N_4 as the photocatalyst, and only a slight decrease can be found for CdS. The TON value for CdS was up to 6.8. Interestingly, g-C_3N_4 contribute to a rather stable photocatalytic performance towards the trifluoromethylation of (hetero)arenes. The crystal structures of these photocatalysts before and after 5 reaction cycles were further revealed by XRD patterns. It is obvious that the diffraction peaks of fresh CdS and g-C_3N_4 can be assigned to hexagonal CdS phase and graphite phase by comparing with the standard data from JCPDS card (File No. 41-1049 and 87–1526), respectively (Fig. 7b, c) [45,46]. All peaks appeared in the recycled CdS and g-C_3N_4 generally match the standard phases of fresh CdS and g-C_3N_4, suggesting that the crystallization and crystallite size of these catalysts are not changed by visible light irradiation.
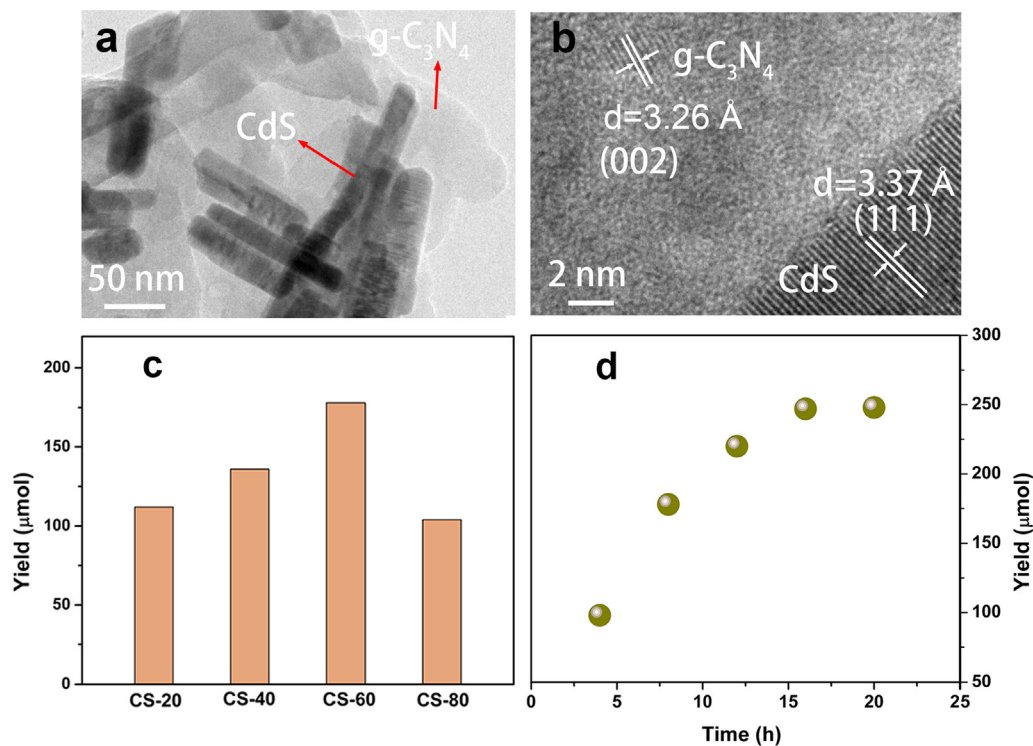
Fig. 6. TEM (a), HRTEM (b) image for CS-60. (c) Yields of **3a** using different catalysts for 8 h. (d) The influence of irradiation time on the amount of **3a**.
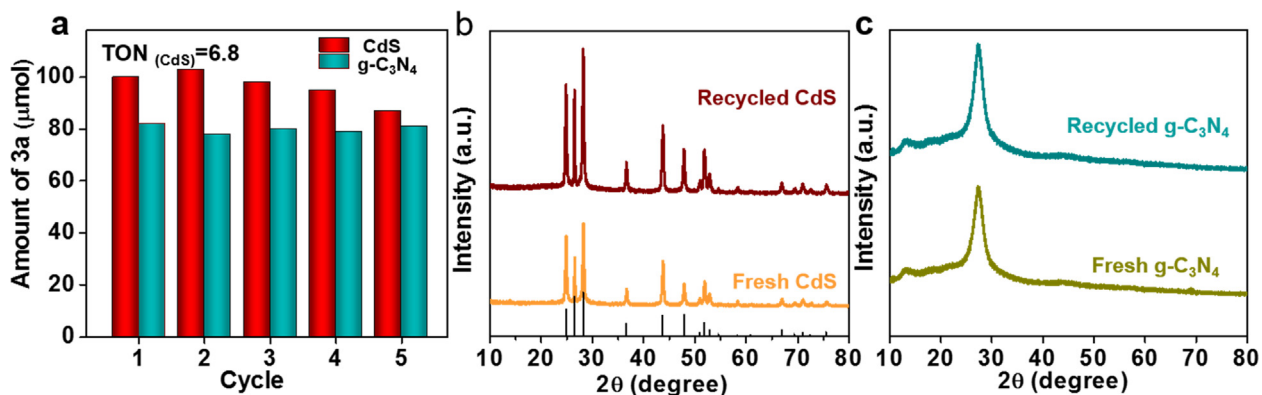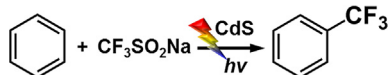

Fig. 7. (a) The recycle experiments of CdS and g-C$_3$N$_4$. (b, c) XRD patterns of fresh CdS and recycled CdS for five cycles.

Table 3
Radical trapping experiments.

Entry	Addictive	Amount of 3a (μmol)
1	none	109
2	TEMPO (2 equiv)	<1

Reaction conditions: 1a (11.2 mmol), 2a (0.5 mmol), CH$_3$CN (1 mL), photocatalyst (20 mg), air atmosphere, light intensity (80 mW/cm^2, λ = 500 nm), irradiation time (12 h), room temperature (25 °C), air atmosphere (0.1 MPa), TEMPO = 2,2,6,6-tetramethylpiperidine-N-oxyl, GC yields.

3.4. Reaction mechanism investigation

Addition of tetramethylpiperidine N-oxide (TEMPO, 2 equiv), a typical radical scavenger, to the standard reaction system significantly lower the yield of **3a** (Table 3). This coupling with the evidence of achieving MNP-CF$_3$ adduct in radical trapping experiment leads to the confirmation of a radical dominant pathway for the trifluoromethylation reactions of (hetero)arenes over CdS or g-C$_3$N$_4$ photocatalyst. The radical involving steps focusing on ·CF$_3$ over solid g-C$_3$N$_4$ surface was also studied by DFT calculations. The top and side views of g-C$_3$N$_4$ structures and the corresponding complex structures with various species (C$_6$H$_6$, CF$_3$, C$_7$H$_5$F$_3$, H) involved in the trifluoromethylation reaction adsorbed on g-C$_3$N$_4$ are optimized (Fig. S3). The calculated free energy diagrams of trifluoromethylation reaction through the above reaction
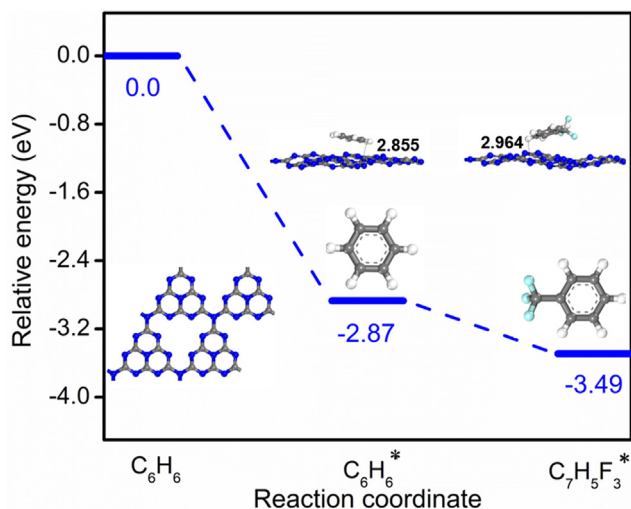
Fig. 8. The E_{ads} of species involved in trifluoromethylation of benzene with g-C_3N_4, inset was the optimized structures of species adsorbed on the monolayer g-C_3N_4.

path on g-C_3N_4 is summarized in Fig. 8. The negative E_{ads} indicates that the adsorption is an exothermic process in all instances. The Eads values of adsorbates are all larger than 1 eV, which indicates the strong chemisorption of these species on g-C_3N_4. The thermodynamic profile shows that the formation of $C_7H_5F_3$ along the step ($C_6H_6^*$+CF_3^* $C_7H_5F_3^*$+H^*) undergoes an energy release process. Additionally, a competitive experiment with the same amounts of benzene and C_6D_6 (1a-d6) in the presence of CdS or g-C_3N_4 was then carried out under visible light irradiation. The kinetic isotopic effect of benzene showed a low K_H/K_D value of 1.0 for the transformation, suggesting that the cleavage of C-H bond in benzene was not the rate-determining step (Fig. 9).
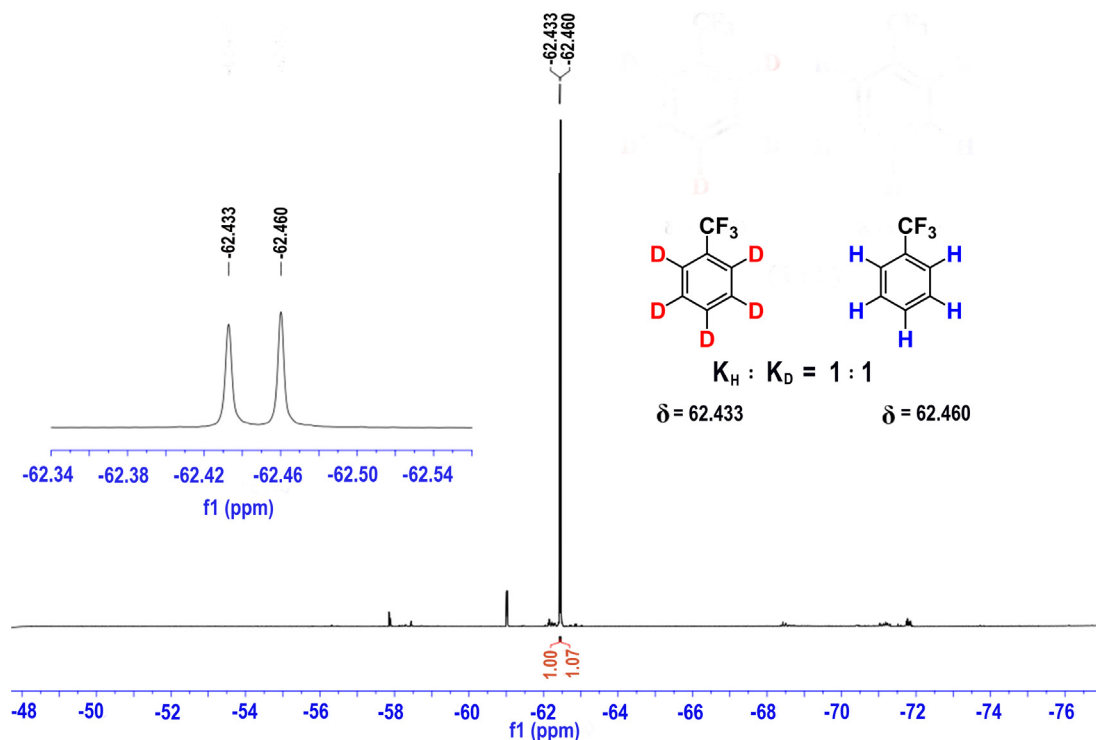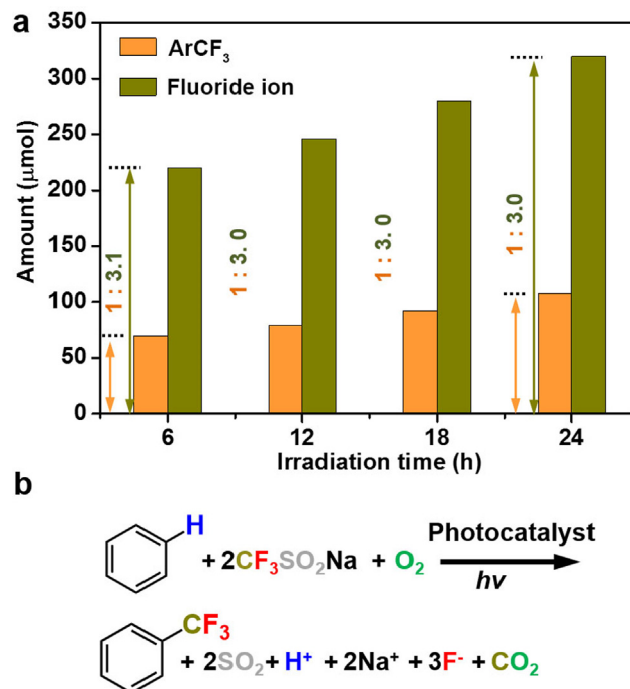

Fig. 10. Influence of irradiation time on the amount of benzotrifluoride and fluorine anion (a). The chemical equation of the trifluoromethylation reaction (b).

Based on the above experimental and DFT results, we then shifted our attention to the activation mechanism of CF_3SO_2Na under O_2 atmosphere during the trifluoromethylation reaction. After light irradiation, F^- and 3a were detected in the ion chromatography spectrum and the ^{19}F NMR spectrum, respectively. The amounts of F^- and 3a increased along with the extending

Fig. 9. KIE experiment.

Table 4
One-pot synthesis of trifluoromethylated anilines from nitro aromatic compound[a].
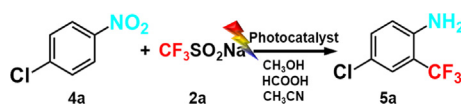
Entry	Substrate	Photocatalyst	Product	Amount (μmol)	Yield (%)
1[a]	4a	CdS	5a	115[c]	23
2	4a	g-C$_3$N$_4$	5a	50	10
3[b]	4a	CdS	5a	–	–

[a] Reaction conditions: 4a (0.2 mmol), 2a (0.5 mmol), CH$_3$CN (1 mL), MeOH (1.5 mmol), formic acid (1.5 mmol), photocatalyst (10 mg), light intensity (500 mw/cm^2, λ = 420–780 nm), irradiation time (24 h), room temperature (25 °C), N$_2$ atmosphere (0.1 MPa). ^{19}F NMR yields with trifluoromethoxybenzene as internal standard.
[b] Without MeOH or formic acid.
[c] 59 μmol p-chloroaniline as by-product also detected.

irradiation time with a growth rate ratio of 3:1, indicating that F$^-$ and benzotrifluoride were the final chemical form of F elements in CF$_3$SO$_2$Na after the transformation (Fig. 10a). When the gas phase reaction mixture was measured on GC–MS, SO$_2$ and CO$_2$ were detected while none of them were found in the absence of CF$_3$SO$_2$Na (Fig. S4). No SO$_4^{2-}$ was detected by the ion chromatography, thus the formation of SO$_4^{2-}$ was ruled out. This was different from the result we have reported using photoexcited quinones as the catalyst in the photocatalytic trifluoromethylation of (hetero) arenes, in which CF$_3$SO$_2$Na transformed into final inorganic product S$_2$O$_4^{2-}$, followed by a classical hydrolyzation reaction to give SO$_4^{2-}$ in the presence of H$_2$O and O$_2$ [24]. According to the above evidences, the whole chemical equation was given in Fig. 10b. This process catalyzed by semiconductor having a strong reductive ability exhibited a lower efficiency in F element utilization than quinones with strong oxidation.

On the basis of all the aforementioned mechanistic investigation, a plausible mechanism for photo-driven semiconductor catalyzed trifluoromethylation of (hetero)arenes using CF$_3$SO$_2$Na as the ·CF$_3$ source is proposed (Scheme 1a). Upon excitation, the photo-generated hole in the valence band of semiconductor oxidized the CF$_3$SO$_2^-$ into ·CF$_3$ and SO$_2$, which is the initiation step of the reaction. Then the ·CF$_3$ followed two reaction pathways as shown in Scheme 1. The electron-deficient ·CF$_3$ attacks on the electron-rich position of (hetero)arenes to produce the key intermediate of trifluoromethyl-cyclohexadienyl radical via electrophilic aromatic substitution (S$_E$Ar). In this process, more than one electron-rich site in the substrates coupled with the steric hindrance effect of the substituent group resulted in low regioselectivity of some reactions. Finally, the formed intermediate was oxidized by the separated hole, followed by the deprotonization process to give the desired benzotrifluoride. Alternatively, the ·CF$_3$ reacted with O$_2^-$ and electrons giving F$^-$ and CO$_2$, which result in a low utilization efficiency of CF$_3$SO$_2$Na. This photocatalytic strategy tolerates oxidative reaction mode using O$_2$ as the electron acceptor [25]. During this process, the photo-generated electrons made no direct contribution to the activation of the substrate or participation in yielding the desired product. One can expect that, once a suitable reductive half-reaction process was introduced into this system, a full utilization of the photo-generated electron-hole pairs rather than using the holes only will be realized. Thus, a trifluoromethylation reaction using nitroaromatic compound as the substrate to synthesize trifluoromethylated anilines was designed to testify this rational speculation (Scheme 1b).

Trifluoromethylated anilines as the core pharmaceutical intermediates have attracted many interests [47]. Current strategies for the synthesis of them mainly use amines as the substrate in the presence of strong acids or bases to protect the amino group which makes the transformation more complicated. We proposed a one-pot synthesis of trifluoromethylated anilines from nitro aromatic compound under mild reaction conditions without functional group protection process. When using the trifluoromethylation of 4-chloronitrobenzene (4a) as the model reaction, CdS and g-C$_3$N$_4$ gave 23% and 10% yield of 2-trifluoromethyl aniline (5a) expectively
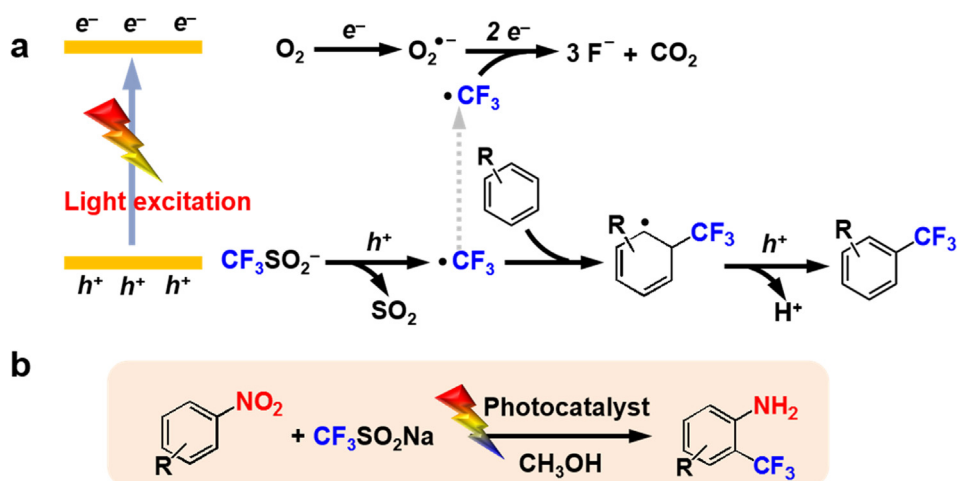
Scheme 1. Proposed mechanism of the trifluoromethylation reaction.

in the presence of CH$_3$OH and formic acid under visible light irradiation for 24 h (Table 4, entries 1–2). As an initial attempt, the transformation hardly proceeded in the absence of CH$_3$OH or formic acid (Table 4, entry 3), which indicates the complicity of this multiphase reaction. Nitro compound was reduced to aromatic amine [48,49] by photo-generated electrons, avoiding the decomposition reaction of ·CF$_3$ radical by O$_2^-$. As shown in Fig. S5, 4-Chloroaniline as main reductive by-product was found with a yield of 59 μmol determined by GC analysis. However, non-reduction product was hardly detected. It is probably because —NO$_2$ was easy to reduce as —NH$_2$ in this reaction system.

4. Conclusions

We have developed a reliable route for direct C—H trifluoromethylation reaction of (hetero)arenes with a broad substrate scope through CdS or g-C$_3$N$_4$ initiated photocatalysis by using CF$_3$-SO$_2$Na to provide ·CF$_3$ radicals. The experimental results revealed the unwanted side reaction of O$_2^-$ with ·CF$_3$ to form CO$_2$ and F$^-$, which limited the effective utilization of CF$_3$SO$_2$Na in photocatalytic synthesis. Furthermore, one-pot synthesis of trifluoromethylated anilines using nitro aromatic compound and CF$_3$SO$_2$Na as the multifunctional substrates has been provided to utilize photogenerated electron-hole pairs simultaneously in one reaction. The understanding of the reaction mechanism of CF$_3$SO$_2$Na in the semiconductor catalyzed reactions helps us to further design new classes of synthetic organic reactions relative to ·CF$_3$ in photocatalytic mode.

Declaration of Competing Interest

The authors declare that they have no known competing financial interests or personal relationships that could have appeared to influence the work reported in this paper.

Acknowledgments

Appendix A. Supplementary material

Supplementary data to this article can be found online at https://doi.org/10.1016/j.jcat.2020.06.032.

References

[1] T. Furuya, A.S. Kamlet, T. Ritter, Nature 473 (2011) 470–477.
[2] C. Le, T.Q. Chen, T. Liang, P. Zhang, D.W.C. MacMillan, Science 360 (2018) 1010–1014.
[3] X. Liu, C. Xu, M. Wang, Q. Liu, Chem. Rev. 115 (2015) 683–730.
[4] E.J. Cho, T.D. Senecal, T. Kinzel, Y. Zhang, D.A. Watson, S.L. Buchwald, Science 328 (2010) 1679–1681.
[5] N.D. Ball, J.W. Kampf, M.S. Sanford, J. Am. Chem. Soc. 132 (2010) 2878–2879.
[6] Y. Ye, S.A. Künzi, M.S. Sanford, Org. Lett. 14 (2012) 4979–4981.
[7] I. Ghosh, J. Khamrai, A. Savateev, N. Shlapakov, M. Antonietti, B. König, Science 365 (2019) 360–366.
[8] M. Hiroki, S. Terajima, T. Shishido, ACS Catal. 8 (2018) 6246–6254.
[9] D.D. Beattie, A.C. Grunwald, T. Perse, L.L. Schafer, J.A. Love, J. Am. Chem. Soc. 140 (2018) 12602–12610.
[10] Y. Ji, T. Brueckl, R.D. Baxter, Y. Fujiwara, I.B. Seiple, S. Su, D.G. Blackmond, P.S. Baran, PNAS 108 (2011) 14411–14415.
[11] A. Studer, Angew. Chem. Int. Ed. 51 (2012) 8950–8958.
[12] L.L. Zhao, P.H. Li, X.Y. Xie, L. Wang, Org. Chem. Front. 5 (2018) 1689–1697.
[13] L. Li, X.Y. Mu, W.B. Liu, Y.C. Wang, Z.T. Mi, C.J. Li, J. Am. Chem. Soc. 138 (2016) 5809–5812.
[14] D.A. Nagib, D.W.C. MacMillan, Nature 480 (2011) 224–228.
[15] E. Torti, S. Protti, M. Fagnoni, Chem. Commun. 54 (2018) 4144–4147.
[16] P. Liu, W.B. Liu, C.J. Li, J. Am. Chem. Soc. 139 (2017) 14315–14321.
[17] Y. Tong, H. Pan, W. Huang, et al., New J. Chem. 43 (2019) 8741–8745.
[18] O.A. Tomashenko, V.V. Grushin, Chem. Rev. 111 (2011) 4475–4521.
[19] N.J.W. Straathof, H.P.L. Gemoets, X. Wang, J.C. Schouten, V. Hessel, T. Noël, ChemSusChem 7 (2014) 1612–1617.
[20] A.K. Pal, C.F. Li, G.S. Hanan, E. Zysman-Colman, Angew. Chem. Int. Ed. 57 (2018) 1–6.
[21] N.J.W. Straathof, S.E. Cramer, V. Hessel, T. Noël, Angew. Chem. Int. Ed. 55 (2016) 15549–15553.
[22] S.P. Pitre, C.D. McTiernan, H. Ismaili, J.C. Scaiano, ACS Catal. 4 (2014) 2530–2535.
[23] N.J.W. Straathof, D.J.G.P. van Osch, A. Schouten, X. Wang, J.C. Schouten, V. Hessel, T. Noël, J. Flow Chem. 4 (2014) 12–17.
[24] B. Chang, H.G. Shao, P. Yan, W.Z. Qiu, Z.Q. Weng, R.S. Yuan, ACS Sustain. Chem. Eng. 5 (2017) 334–341.
[25] J. Lin, Z. Li, J. Kan, S.J. Huang, W.P. Su, Y.D. Li, Nat. Commun. 8 (2016) 14353.
[26] M. Baar, S. Blechert, Chem. Eur. J. 21 (2015) 526–530.
[27] M. Zhao, H. Xu, H. Chen, S. Ouyang, N. Umezawa, D. Wang, J. Ye, J. Mater. Chem. A 3 (2015) 2331–2337.
[28] J. Tauber, D. Imbri, T. Opatz, Molecules 19 (2014) 16190–16222.
[29] H. Morimoto, T. Tsubogo, N.D. Litvinas, J.F. Hartwig, Angew. Chem. 123 (2011) 3877–3882.
[30] M.A. García-Monforte, S. Martínez-Salvador, B. Menjón, Eur. J. Inorg. Chem. 2012 (2012) 4945–4966.
[31] T. Kino, Y. Nagase, Y. Ohtsuka, K. Yamamoto, D. Uraguchi, K. Tokuhisa, T. Yamakawa, J. Fluorine Chem. 131 (2010) 98–105.
[32] H.W. Huang, B. Pradhan, J. Hofkens, M.B.J. Roeffaers, J.A. Steele, ACS Energy Lett. 5 (2020) 1107–1123.
[33] A. Dalui, M. Pandey, P.K. Sarkar, B. Pradhan, A. Vasdev, N.B. Manik, G. Sheet, S. Acharya, ACS Appl. Mater. Interfaces 11 (2019) 11749–11754.
[34] J.P. Perdew, K. Burke, M. Ernzerhof, Phys. Rev. Lett. 77 (1996) 3865.
[35] A. Bergner, M. Dolg, W. Küchle, H. Stoll, H. Preuß, Mol. Phys. 80 (1993) 1431–1441.
[36] C.-S. Lee, T.-S. Hwang, Y. Wang, S.-M. Peng, C.-S. Hwang, J. Phys. Chem. 100 (1996) 2934–2941.
[37] J.T. Li, N.Q. Wu, Catal. Sci. Technol. 5 (2015) 1360–1384.
[38] S.M. Goodman, M. Levy, F.F. Li, Y.C. Ding, C.M. Courtney, P.P. Chowdhury, A. Erbse, A. Chatterjee, P. Nagpal, Front. Chem. 6 (2018) 46.
[39] D. Dvoranová, Z. Barbieriková, V. Brezová, Molecules 19 (2014) 17279–17304.
[40] Y.-W. Jun, S.-M. Lee, N.-J. Kang, J. Cheon, J. Am. Chem. Soc. 123 (2001) 5150–5151.
[41] Y.C. Liang, T.W. Lung, Nanoscale Res. Let. 11 (2016) 1–11.
[42] J. Yu, C. Gong, Z. Wu, Y. Wu, W. Xiao, Y. Su, L. Sun, C.J. Lin, J. Mater. Chem. A 3 (2015) 22218–22226.
[43] W. Zhang, L. Zhou, H. Deng, J. Mater. Chem. A 423 (2016) 270–276.
[44] E. Vorobyeva, Z. Chen, S. Mitchell, R.K. Leary, P. Midgley, J.M. Thomas, R. Hauert, E. Fako, N. López, J. Pérez-Ramírez, J. Mater. Chem. A 5 (2017) 16393–16403.
[45] H.Q. Cao, G.Z. Wang, S.C. Zhang, X.R. Zhang, D. Rabinovich, Inorg. Chem. 45 (2006) 5103–5108.
[46] J. Ma, C. Wang, H. He, Appl. Catal. B-Environ. 184 (2016) 28–34.
[47] X.Y. Gao, Y. Geng, S.J. Han, A. Liang, J.G. Li, D.P. Zou, Y.S. Wu, Y.J. Wu, Org. Lett. 20 (2018) 3732–3735.
[48] T. Cuypers, P. Tomkins, D.E. De Vos, Catal. Sci. Technol. 8 (2018) 2519–2523.
[49] S. Li, F. Wang, Y. Liu, Y. Cao, Chin. J. Chem. 35 (2017) 591–595.